Journal of
Translational Regenerative Medicine

2026. Volume 1

Research Paper

Optimizing 3D Bioprinting Parameters for Alginate-graphene Oxide Bioinks in Cardiac Tissue Engineering

Fatemeh Edrisi[1], Nafiseh Baheiraei[2*], Ali Zamanian[3*]

1. Department of Modern Technologies in the Engineering, Faculty of Interdisciplinary Science and Technology, Tarbiat Modares University, Tehran, Iran.
2. Tissue Engineering and Applied Cell Sciences Division, Department of Anatomical Sciences, Faculty of Medical Sciences, Tarbiat Modares University, Tehran, Iran.
3. Department of Nanotechnology and Advanced Materials, Materials and Energy Research Center (MERC), Karaj, Iran.

Use your device to scan and read the article online

Citation Edrisi F, Baheiraei N, Zamanian A. Optimizing 3D Bioprinting Parameters for Alginate-graphene Oxide Bioinks in Cardiac Tissue Engineering. Journal of Translational Regenerative Medicine. 2025; 1:E1000. http://dx.doi.org/10.32598/JTRM.1.1000

http://dx.doi.org/10.32598/JTRM.1.1000

ABSTRACT

Background: Three-dimensional (3D) bioprinting presents a promising platform for fabricating tissue-engineered scaffolds with controlled architecture and cellular integration.

Methods: In this study, alginate (Alg)-based bioinks incorporating varying concentrations of graphene oxide (GO) were evaluated to optimize key bioprinting parameters (Alg concentration, nozzle diameter, and extrusion pressure) for cardiac tissue engineering applications. Bioinks were formulated with 6%, 7%, and 8% (w/v) Alg and GO concentrations ranging from 0 to 2.0 mg/mL. Printability and structural fidelity were assessed using multiple nozzle sizes (22 G and 25 G) and extrusion pressures (0.85–1.4 bar).

Results: Results indicated that an Alg concentration of 8% provided superior viscosity and shape retention. The 22-G nozzle offered an optimal balance between filament continuity and pore morphology. GO incorporation resulted in thinner filaments and larger pores, with optimal extrusion pressures varying according to GO concentration.

Conclusion: These findings provide a framework for tailoring bioprinting parameters to improve scaffold performance and effectiveness in cardiac tissue engineering.

Keywords: 3D bioprinting, Cardiac tissue engineering, Alginate (Alg), Graphene oxide (GO)

Article info:
Received: 23 Sep 2025
Accepted: 27 Oct 2025
Publish: 10 Jan 2026

*** Corresponding Authors:**
Nafiseh Baheiraei, Associate Professor.
Address: *Tissue Engineering and Applied Cell Sciences Division, Department of Anatomical Sciences, Faculty of Medical Sciences, Tarbiat Modares University, Tehran, Iran.*
E-mail: *n.baheiraei@modares.ac.ir*

Ali Zamanian, Professor.
Address: *Department of Nanotechnology and Advanced Materials, Materials and Energy Research Center (MERC), Karaj, Iran.*
E-mail: *a-zamanian@merc.ac.ir*

Highlights

- The 8% Alg bioink showed superior viscosity and shape fidelity.
- The 22-G nozzle achieved optimal filament continuity and pore morphology.
- GO incorporation provided thinner filaments and larger pores.
- Extrusion pressure requirements vary based on GO concentration

Plain Language Summary

Heart disease is a major health problem, and scientists are looking for new ways to repair damaged heart tissue. One promising method is 3D bioprinting, which works like a printer but uses special materials called "bioinks" to build tiny structures that can support living cells and heart tissue. In this study, we tested bioinks made from alginate (Alg), a natural material from seaweed, mixed with graphene oxide (GO), a carbon-based additive. We aimed to find the best printing conditions—such as the bioink thickness, nozzle size, and applied pressure—under which the printed structures would be strong and retain their shape. We found that bioinks with 8% Alg worked better and a 22-G nozzle gave the most reliable results. Adding GO changed the structure by making filaments thinner and pores larger. These results show how adjusting printing conditions can improve scaffold quality, bringing us closer to building tissues that may one day help patients with heart disease.

Introduction

Tissue-engineered constructs offer valuable platforms for in vitro investigation and serve as potential substitutes for diseased or impaired tissues. As a rapidly advancing technology, three-dimensional (3D) bioprinting facilitates tissue engineering by enabling the spatially controlled deposition of biomaterials and living cells into predefined architectures [1]. Furthermore, 3D bioprinting overcomes the microstructural precision limitations typically associated with conventional manufacturing methods [2]. Among the various 3D bioprinting techniques, extrusion-based printing is the most widely used due to its extensive material versatility, ease of implementation, and adaptability across diverse fabrication environments. Guided by computer-aided design (CAD), this method enables the precise tuning of structural parameters, including pore morphology and distribution [3, 4].

Hydrogels are considered promising bioinks for 3D bioprinting due to their biocompatibility, biodegradability, and structural similarity to the extracellular matrix (ECM). Furthermore, their high water content facilitates efficient diffusion of nutrients and gases, which is vital for maintaining cell viability within printed constructs [5]. The printability of hydrogels is influenced by multiple factors, including their chemical composition, viscosity, and key printing parameters such as nozzle diameter, temperature, pressure, and flow rate [6, 7]. To ensure smooth extrusion during bioprinting, bioinks are generally formulated with low viscosity [8]. However, increasing viscosity and using finer nozzle diameters can significantly improve the resolution of printed constructs. Despite this advantage, these conditions expose encapsulated cells to elevated shear forces during deposition, which may adversely affect their viability and biological function [9]. Moreover, extrusion pressure is a critical parameter in bioprinting, as elevated pressure levels can produce thicker filament strands during deposition. Strand size in bioprinted scaffolds has a significant influence on the survival and growth of embedded cells. Thicker strands can impede the transport of essential nutrients and oxygen, resulting in suboptimal cellular function [10, 11]. Therefore, careful optimization of these variables is essential for achieving high-quality printed constructs and promoting favorable cellular outcomes.

Among naturally sourced hydrogels, alginate (Alg), a polysaccharide derived from brown algae, is recognized as one of the most frequently utilized materials in bioprinting applications [12] due to its favorable biocompatibility, non-toxicity, ECM-like physical structure, rapid gelation modulated by divalent cations such as calcium and barium, high aqueous solubility, and low cost [13-15]. However, its limited mechanical strength, poor

print fidelity, and lack of intrinsic bioactive motifs for cell adhesion and differentiation remain significant challenges in tissue engineering [16, 17]. Filler nanomaterials, such as carbon-based nanomaterials, play a pivotal role in modulating both the structural and physicochemical properties of printed hydrogels. In addition to enabling customization of scaffold architecture, these additives significantly influence the rheological behavior of bioinks during the bioprinting process. Consequently, their incorporation can directly impact the fidelity, resolution, and overall quality of the final printed scaffold [18-20]. Graphene oxide (GO), a type of carbon-based nanomaterial, contains functional groups such as carboxyl, hydroxyl, and epoxy. These groups enable strong molecular interactions, which enhance the mechanical properties of GO-incorporated hydrogels compared to those without GO [21]. As a result, incorporating GO into Alg hydrogels can enhance both their mechanical strength and printability [22]. This study aims to optimize key 3D printing parameters to fabricate scaffolds with structural and functional properties suitable for tissue engineering applications.

Materials and Methods

Preparation of bioinks

To prepare the bioinks, 6%, 7%, and 8% (w/v) sodium Alg (W201502, Sigma-Aldrich) were dissolved in deionized water and vortexed for 20 minutes to ensure complete dissolution. The resulting Alg solutions were then combined with varying concentrations of GO dispersions at 0, 0.05, 0.1, and 2.0 mg/mL (Graphene X, Iran). The mixtures were stirred continuously for an additional 20 minutes to promote the uniform distribution of GO within the hydrogel matrix.

3D printing process for scaffold construction

Following preparation, the bioink was loaded into the syringe reservoir of an extrusion-based 3D bioprinter N2 (3DPL Co. Ltd., Tehran, Iran), equipped with 3-axis motion control (x, y, and z) and a pneumatic extrusion system operating at pressures below 2 bar. Cube-shaped scaffold models (20×20 mm, 5 layers) were designed using AutoCAD software. The resulting geometries were exported in STL format and subsequently converted into G-code using Simplifier software to enable 3D printing. All samples were printed at room temperature with a consistent printing speed of 60 mm/s [23]. Figure 1 demonstrates the bioprinting process.

Optimization of key 3D bioprinting parameters

To enhance the printability, mechanical stability, and geometric precision of the Alg-GO constructs, critical 3D bioprinting parameters, including hydrogel concentration, extrusion pressure, and needle diameter, were optimized. To determine the optimal Alg concentration, 3D bioprinting was conducted using Alg solutions at 6%, 7%, and 8% (w/v), each combined with varying GO concentrations (0, 0.05, 0.1, and 2 mg/mL). The complete set

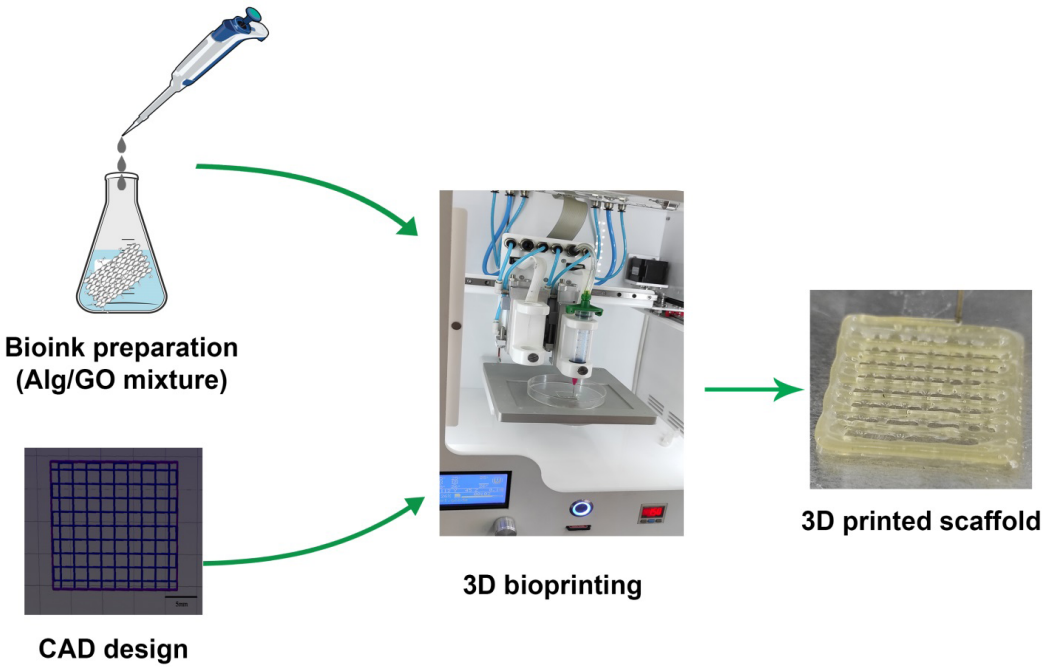

Figure 1. Illustration of the bioprinting process

Table 1. Constituents of the formulated bioinks

Sample Name	Alg (% w/v)	GO (mg/mL)
Alg6-GO-0	6	0
Alg6-GO-1	6	0.05
Alg6-GO-2	6	0.1
Alg6-GO-3	6	0.2
Alg7-GO-0	7	0
Alg7-GO-1	7	0.05
Alg8-GO-0	8	0
Alg8-GO-1	8	0.05
Alg8-GO-2	8	0.1
Alg8-GO-3	8	0.2

of bioink formulations is summarized in Table 1. Subsequently, to address the optimal nozzle diameter, the bioprinting process was performed using 22-G and 25-G nozzles exclusively with the optimized concentration of Alg, i.e. the Alg8-GO-0 formulation. Following this, the Alg8-GO-0, Alg8-GO-1, Alg8-GO-2, and Alg8-GO-3 formulations were bioprinted using the optimized nozzle diameter, while varying the extrusion pressure between 0.85 and 1.4 bars to identify the most suitable pressure for each sample.

Statistical analysis

All experiments were done three times, and the results are shown accordingly.

Results

Bioprinted Alg-based scaffolds often suffer from poor shape fidelity due to insufficient viscosity. Increasing Alg concentration enhanced viscosity and improved structural stability during printing. As illustrated in Figure 2, the 6% Alg formulation (Alg6-GO-0) exhibited acceptable printability. However, upon incorporating GO, the bioinks failed to maintain adequate structural integrity post-extrusion. Subsequently, the Alg concentration was increased to 7%, and the 3D bioprinting process was repeated. As expected, the Alg7-GO-0 formulation demonstrated acceptable printability; however, Alg7-GO-1 exhibited poor structural uniformity and integrity (Figure 2). Consequently, further printing with Alg7-GO-2 and Alg7-GO-3 at the same concentration was not pursued. In the next phase, samples Alg8-GO-0, Alg8-GO-1, Alg8-GO-2, and Alg8-GO-3 were successfully bioprinted, all displaying satisfactory printability and shape fidelity following the extrusion process (Figure 2). Based on these results, a concentration of 8% was identified as the optimal formulation in this study, providing superior printability and structural integrity compared to lower concentrations.

Printing Alg8-GO-0 with a 25-G nozzle required substantially higher pressure (>1 bar) due to its smaller inner diameter, resulting in thinner filaments and larger pores. The extrusion process lacked continuity, and the hydrogel was deposited discontinuously (Figure 3a). The incorporation of GO particles further exacerbated this issue. These findings indicate that the 25-G nozzle is unsuitable for this application. In contrast, printing with the 22-G nozzle required lower pressure (<1 bar), produced slightly thicker filaments, and yielded smaller pores (Figure 3b). The extrusion process exhibited acceptable continuity, suggesting that the 22-G nozzle offers a more favorable balance between pressure requirements and print quality.

In the next stage, various extrusion pressures were evaluated across four groups to identify the optimal pressure that provides the highest printing resolution. For Alg8-GO-0, an initial pressure of 0.99 bar produced continuous ink flow but resulted in excessive strand thickness, leading to partial pore closure. Reducing the pressure to 0.85 bar improved both filament diameter and pore uniformity, establishing it as the optimal setting for this group (Figure 4). Alg8-GO-1, initially printed at 0.85 bar, produced thinner strands and larger pores compared to Alg8-GO-0, although continuity was slightly compromised in some

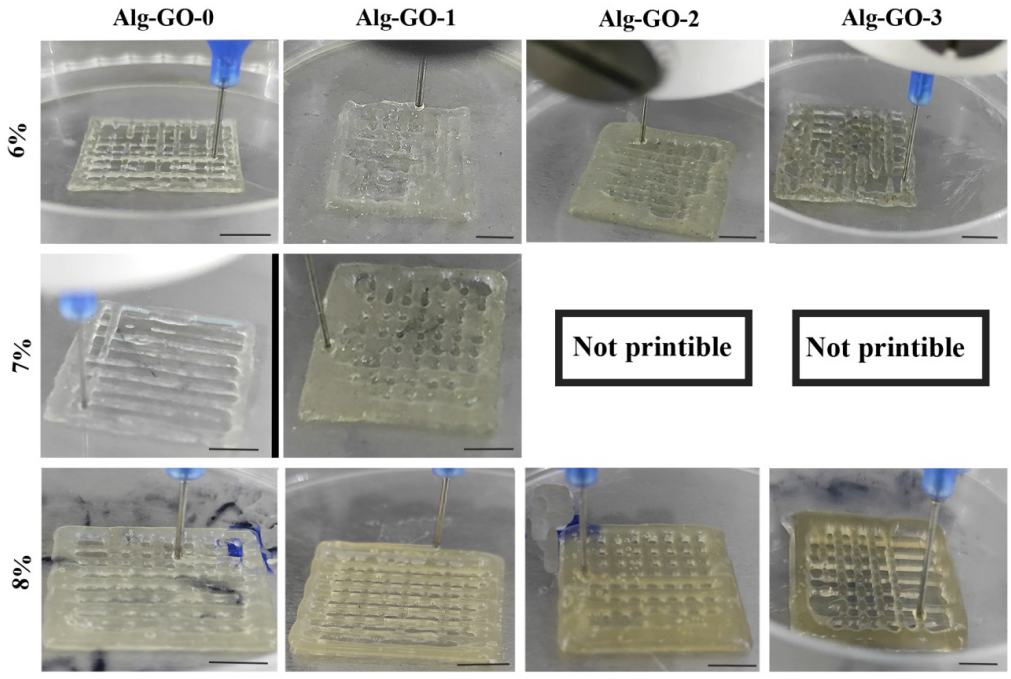

Figure 2. Poor printability of Alg 6% and 7% samples and acceptable printability of Alg 8%

Note: As shown, the resulting structures with Alg formulations at 6% and 7% concentrations exhibited a lack of uniformity and continuity. In contrast, the 8% Alg sample exhibited markedly improved printability, suggesting enhanced shape fidelity during the extrusion process (scale bar: 0.5 cm).

regions. To refine pore size, the pressure was increased to 0.99 bar and then to 1.10 bar; however, inadequate ink flow prompted a further adjustment to 1.25 bar, which yielded structurally acceptable scaffolds and was deemed optimal (Figure 4). For Alg8-GO-2, 0.85 and 0.99 bar pressures were insufficient due to low ink flow and nozzle clogging, probably caused by high surface adhesion forces [24]. At 1.25 bar, consistent flow and desirable strand morphology were achieved (Figure 4). Alg8-GO-3 could not be printed at 0.85 bar, and printing at 0.99 bar resulted in undesirable scaffold features. Ultimately, 1.25 bar was selected, with a mid-process increase to approximately 1.4 bar to overcome nozzle blockage and ensure consistent strand deposition (Figure 4).

Discussion

The results highlight the importance of optimizing bioink composition and printing parameters for cardiac tissue engineering. Increasing Alg concentration improved viscosity and shape fidelity, with 8% Alg providing the most stable scaffolds by increasing the number of

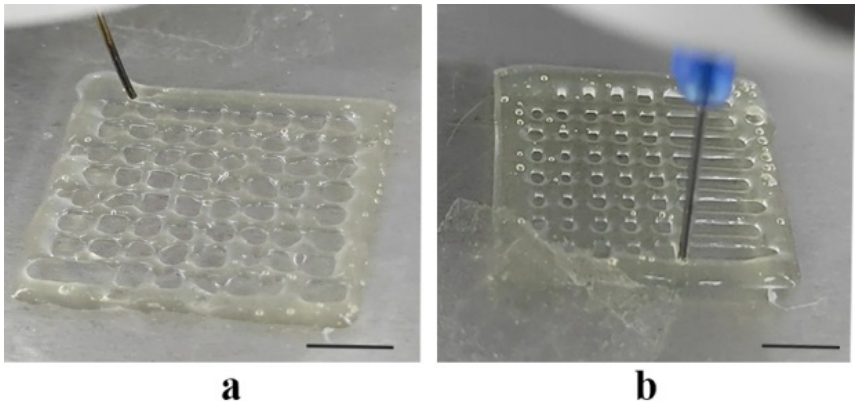

Figure 3. Structural difference between printed scaffolds with a 25-G needle (a) and a 22-G needle (b)

Note: Satisfactory uniformity and continuity in the printing of scaffold B were observed (scale bar: 0.5 cm).

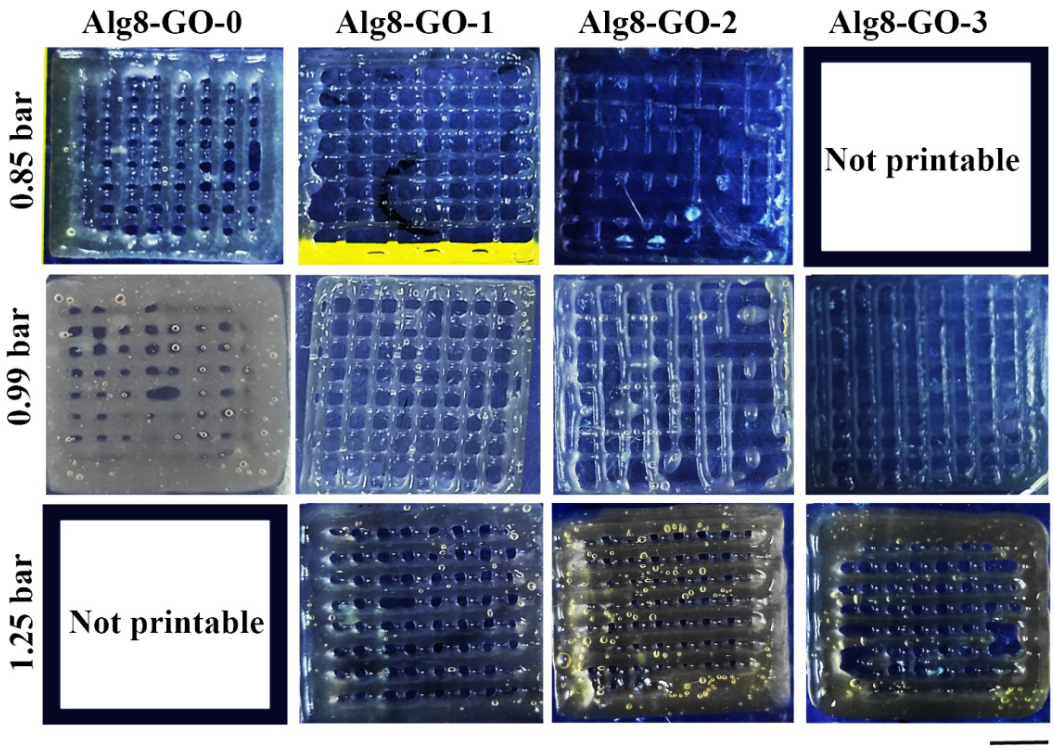

Figure 4. Printed scaffolds under varying extrusion pressures and the influence of GO concentration on filament morphology

Note: Optimal printing pressure for each scaffold formulation depends on the specific GO content (scale bar: 0.5 cm).

G-blocks, thereby enhancing structural stability during printing [6]. Lower concentrations were insufficient, particularly when GO was incorporated. This may be attributed to the reduced viscosity of the Alg hydrogel observed after incorporating low GO concentrations (<0.2 mg ml^{-1}), may be due to the homogeneous and parallel alignment of GO sheets along the Alg polymer chains without contacting each other [25].

As mentioned before, nozzle diameter is a critical parameter in the 3D bioprinting process. The filament width and pore size of the printed constructs are directly influenced by the nozzle's inner diameter [26]. In our study, the 25-G nozzle produced discontinuous filaments and was prone to clogging at the nozzle tip, especially with GO sheets, making it unsuitable. The 22-G nozzle offered a better balance between extrusion pressure and print quality. When cells are present in the bioink, a larger nozzle diameter is preferable, as previous studies on cell-laden Alg hydrogel bioprinting have shown that larger nozzle diameters result in higher cell viability [27]. This improvement is likely due to reduced shear stress, which otherwise adversely affects the viability of encapsulated cells when small-diameter nozzles are used [9].

Extrusion pressure optimization is formulation-dependent. Excessive extrusion pressure generally produces thick strands, while insufficient pressure may result in irregular filament deposition [20, 28]. Additionally, the incorporation of GO into Alg hydrogels results in the formation of thinner filaments and larger pores, likely due to enhanced molecular interactions between Alg and GO [20]. This phenomenon becomes particularly significant when bioinks are cell-laden, as the dimensions of printed strands directly influence the viability and proliferation of encapsulated cells. For example, thicker filaments may hinder the diffusion of essential nutrients and oxygen, potentially compromising cell survival within the scaffold [10, 11]. Consequently, identifying the optimal extrusion pressure for each formulation, based on nozzle diameter and bioink viscosity, is crucial for ensuring structural accuracy in 3D bioprinting.

Conclusion

This study demonstrates that fine-tuning Alg concentration, nozzle diameter, and extrusion pressure is essential for achieving structurally robust and biologically viable scaffolds in 3D bioprinting. An 8% Alg formulation combined with GO enhances printability and mechanical integrity. The 22G nozzle was identified as optimal

for maintaining filament continuity and pore uniformity, while extrusion pressures between 0.85 and 1.25 bar produced the most consistent scaffold architecture across formulations. These insights contribute to the development of customized biofabrication strategies for cardiac tissue engineering applications.

Ethical Considerations

Compliance with ethical guidelines

There were no ethical considerations to be considered in this research.

Funding

This study paper was extracted from the master's thesis of Fatemeh Edrisi, approved by the Department of Modern Technologies in the Engineering, Faculty of Interdisciplinary Science and Technology, Tarbiat Modares University, Tehran, Iran.

Authors' contributions

Conceptualization, and supervision: Nafiseh Baheiraei and Ali Zamanian; Methodology: Nafiseh Baheiraei, Ali Zamanian, and Fatemeh Edrisi; Software, validation, visualization, formal analysis, investigation, data curation, and writing the original draft preparation: Fatemeh Edrisi; Review and editing: Nafiseh Baheiraei and Ali Zamanian; Funding acquisition and resources: Nafiseh Baheiraei.

Conflict of interest

The authors declared no conflict of interest.

References

[1] Li J, Liu X, Crook JM, Wallace GG. Development of 3D printable graphene oxide based bio-ink for cell support and tissue engineering. Frontiers in Bioengineering and Biotechnology. 2022; 10:994776. [DOI:10.3389/fbioe.2022.994776] [PMID]

[2] Zhang B, Cristescu R, Chrisey DB, Narayan RJ. Solvent-based Extrusion 3D Printing for the Fabrication of Tissue Engineering Scaffolds. International Journal of Bioprinting. 2020; 6(1):211. [DOI:10.18063/ijb.v6i1.211] [PMID]

[3] Qasim M, Haq F, Kang MH, Kim JH. 3D printing approaches for cardiac tissue engineering and role of immune modulation in tissue regeneration. International Journal of Nanomedicine. 2019; 14:1311-33. [DOI:10.2147/IJN.S189587] [PMID]

[4] Chen DX. Extrusion Bioprinting of Scaffolds. In: Extrusion Bioprinting of Scaffolds for Tissue Engineering Applications. Cham: Springer; 2019. [DOI:10.1007/978-3-030-03460-3_6]

[5] Das S, Basu B. An overview of hydrogel-based bioinks for 3d bioprinting of soft tissues. Journal of the Indian Institute of Science. 2019; 99(3):405-28. [DOI:10.1007/s41745-019-00129-5]

[6] Khoshnood N, Zamanian A. Development of novel alginate-polyethyleneimine cell-laden bioink designed for 3D bioprinting of cutaneous wound healing scaffolds. Journal of Applied Polymer Science. 2022; 139(21):52227. [DOI:10.1002/app.52227]

[7] Wang J, Hu H, Liu Z, Shi Y, Huang Y. Optimization of 3D Printing Nozzle Parameters and the Optimal Combination of 3D Printer Process Parameters for Engineering Plastics with High Melting Points and Large Thermal Expansion Coefficients. Materials (Basel). 2025; 18(3):500. [DOI:10.3390/ma18030500] [PMID]

[8] Magalhães IP, Oliveira PM, Dernowsek J, Casas EB, Casas MS. Investigation of the effect of nozzle design on rheological bioprinting properties using computational fluid dynamics. Matéria (Rio de Janeiro). 2019; 24(3):e12401. [DOI:10.1590/s1517-707620190003.0714]

[9] Murphy SV, Atala A. 3D bioprinting of tissues and organs. Nature Biotechnology. 2014; 32(8):773-85. [DOI:10.1038/nbt.2958] [PMID]

[10] Kesti M, Müller M, Becher J, Schnabelrauch M, D'Este M, Eglin D, et al. A versatile bioink for three-dimensional printing of cellular scaffolds based on thermally and photo-triggered tandem gelation. Acta Biomaterialia. 2015; 11:162-72. [DOI:10.1016/j.actbio.2014.09.033] [PMID]

[11] Cidonio G, Glinka M, Dawson JI, Oreffo ROC.The cell in the ink: Improving biofabrication by printing stem cells for skeletal regenerative medicine. Biomaterials. 2019; 209:10-24. [DOI:10.1016/j.biomaterials.2019.04.009] [PMID]

[12] Stapenhorst F, dos Santos MG, Prestes JP, Alcantara BJ, Borges MF, Pranke P. Bioprinting: A promising approach for tissue regeneration. Bioprinting. 2021; 22:e00130. [DOI:10.1016/j.bprint.2021.e00130]

[13] Liu S, Li H, Tang B, Bi S, Li L. Scaling law and microstructure of alginate hydrogel. Carbohydrate Polymers. 2016; 135:101-9. [DOI:10.1016/j.carbpol.2015.08.086] [PMID]

[14] Liling G, Di Z, Jiachao X, Xin G, Xiaoting F, Qing Z. Effects of ionic crosslinking on physical and mechanical properties of alginate mulching films. Carbohydrate Polymers. 2016; 136:259-65. [DOI:10.1016/j.carbpol.2015.09.034] [PMID]

[15] Ching SH, Bansal N, Bhandari B. Alginate gel particles-A review of production techniques and physical properties. Critical Reviews in Food Science and Nutrition. 2017; 57(6):1133-52. [DOI:10.1080/10408398.2014.965773] [PMID]

[16] Park J, Lee SJ, Chung S, Lee JH, Kim WD, Lee JY, et al. Cell-laden 3D bioprinting hydrogel matrix depending on different compositions for soft tissue engineering: Characterization and evaluation. Materials Science & Engineering. C, Materials for Biological Applications. 2017; 71:678-84. [DOI:10.1016/j.msec.2016.10.069] [PMID]

[17] Choe G, Park J, Jo H, Kim YS, Ahn Y, Lee JY. Studies on the effects of microencapsulated human mesenchymal stem cells in RGD-modified alginate on cardiomyocytes under oxidative stress conditions using in vitro biomimetic co-culture system. International Journal of Biological Macromolecules. 2019; 123:512-20. [DOI:10.1016/j.ijbiomac.2018.11.115] [PMID]

[18] Athukorala SS, Tran TS, Balu R, Truong VK, Chapman J, Dutta NK, et al. 3D Printable Electrically Conductive Hydrogel Scaffolds for Biomedical Applications: A review. Polymers (Basel). 2021; 13(3):474. [DOI:10.3390/polym13030474] [PMID]

[19] Izadifar M, Chapman D, Babyn P, Chen X, Kelly ME. UV-Assisted 3D Bioprinting of Nanoreinforced Hybrid Cardiac Patch for Myocardial Tissue Engineering. Tissue Engineering. Part C, Methods. 2018; 24(2):74-88. [DOI:10.1089/ten.tec.2017.0346] [PMID]

[20] Choe G, Oh S, Seok JM, Park SA, Lee JY. Graphene oxide/alginate composites as novel bioinks for three-dimensional mesenchymal stem cell printing and bone regeneration applications. Nanoscale. 2019; 11(48):23275-85. [DOI:10.1039/c9nr07643c] [PMID]

[21] Edrisi F, Baheiraei N, Razavi M, Roshanbinfar K, Imani R, Jalilinejad N. Potential of graphene-based nanomaterials for cardiac tissue engineering. Journal of Materials Chemistry. B. 2023; 11(31):7280-99. [DOI:10.1039/D3TB00654A] [PMID]

[22] Li H, Liu S, Li L. Rheological study on 3D printability of alginate hydrogel and effect of graphene oxide. International Journal of Bioprinting. 2016; 2(2):54–66. [DOI:10.18063/IJB.2016.02.007]

[23] Roche CD, Lin H, Huang Y, de Bock CE, Beck D, Xue M, et al. 3D bioprinted alginate-gelatin hydrogel patches containing cardiac spheroids recover heart function in a mouse model of myocardial infarction. Bioprinting. 2023; 30:e00263. [DOI:10.1016/j.bprint.2023.e00263]

[24] Liu HX, Tan YQ, Zhang QX, Qin X, Zheng RR, Sui KY, et al. Rheological behaviors of carbonaceous materials suspended in sodium alginate solutions. Advanced Materials Research. 2014; 906:232-7. [Link]

[25] Pottathara YB, Kokol V. Effect of nozzle diameter and cross-linking on the micro-structure, compressive and biodegradation properties of 3D printed gelatin/collagen/hydroxyapatite hydrogel. Bioprinting. 2023; 31:e00266. [DOI:10.1016/j.bprint.2023.e00266]

[26] Chang R, Nam J, Sun W. Effects of dispensing pressure and nozzle diameter on cell survival from solid freeform fabrication-based direct cell writing. Tissue Engineering. 2008; 14(1):41-8. [DOI:10.1089/ten.a.2007.0004] [PMID]

[27] Ng WL, Lee JM, Yeong WY, Win Naing M. Microvalve-based bioprinting - process, bio-inks and applications. Biomaterials Science. 2017; 5(4):632-47. [DOI:10.1039/C6BM00861E] [PMID]

[28] Passamai VE, Katz S, Alvarez V, Castro GR. Bio-inks for 3D extrusion-based bio-printed scaffolds: Printability assessment. International Journal of Advances in Medical Biotechnology. 2019; 2(1):43-5. [DOI:10.25061/2595-3931/IJAMB/2019.v2i1.43]